OPTIMIZATION OF PROCESSING PARAMETERS DURING ISM PROCESS OF Ti-15-3 ①

Guo Jingjie, Su Yanqing, Liu Yuan, Ren Zhijiang and Jia Jun
School of Materials Science and Engineering,
Harbin Institute of Technology, Harbin 150001, P. R. China

ABSTRACT Based on the direct finite difference method, a numerical model for simulating the temperature field in the charge during Induction Skull Melting (ISM) process has been developed. By use of the simulation program, the temperature field in the charge of Ti-15V-3Cr-3Sn-3Al (Ti-15-3) has been calculated under the condition of various melting powers and charge weights. Furthermore, the relationship between the ultimate temperature in the melt and the melting power, charge weight has been set up. On the basis of the relationship, the parameters during the ISM process of Ti-15-3 (the principle is adaptable to other titanium alloys) would be optimized, consequently, much man-power and finance would be saved and the quality of the melt would be improved.

Key words induction skull melting Ti-15-3 optimization of processing parameters

1 INTRODUCTION

The ISM is one of the best melting process for melting reactive alloys, such as titanium alloys, Ti_3Al-based alloys, TiAl based-alloys and TiNi based-alloys with the function of shape-memory because of its many advantages compared with other melting processes[1-3]. It is a new technique and, at present, is applied only in several advanced countries that have invested much money to study this process[4,5]. However, by now, almost all of the work is concentrated on the experimental research, but from the point of theoretical research, little work has been carried out or reported, for example for the temperature-simulation, only a little work on the ceramic crucible had been carried out[6,9]. So it is very important to conduct some theoretical research on the water-cooled copper crucible adopted in the ISM process, which can save much cost and man-power, at the same time, propel the application of the ISM process in our country.

Ti-15V-3Cr-3Al-3Sn (Ti-15-3), a typical metastable beta-titanium alloy, was developed to answer the need for a titanium alloy sheet in aerospace application[10,11]. This paper begins with the simulation of temperature field in the charge of Ti-15-3 alloy and its aim is to establish the relationship between the melt temperature and the charge weight, the melting power, at last attain the goal of optimization of processing parameters.

2 NUMERICAL MODEL

2.1 Controlling formula

Here are the several conditions to simplify the model:

1) The charge is compact.

2) Power gradients only exist in the radial direction.

Because of the axial-symmetry charge in the cold crucible, a fan shape charge is chosen as the controlling unit that is shown in Fig. 1. It is without doubt that the heat transfer exists in the direction of the radius and the axle. According to the energy conservation theory, the following finite-differential equation can be gotten.

① Project No. 97J18.0.0HT0126 supported by the National Defense Foundation of China
Received Jul. 14, 1998; accepted Sep. 4, 1998

Considering the mutual heat radiation between the charge and the crucible wall, the blackness is

$$\varepsilon = \frac{1}{1/\varepsilon_1 + 1/\varepsilon_2 - 1} \quad (11)$$

where ε_1 —the blackness of charge;

ε_2 —the blackness of cold crucible.

Boundary 4 is the same as boundary 3.

3 TEMPERATURE DISTRIBUTION IN CHARGE

3.1 Key point temperature

Table 1 lists the step-increasing power used for simulative computation. The original charge weight of Ti-15-3 is 4 kg.

Table 1 Exerted power for simulative computation

Time/s	Power/kW
0 ~ 50	50
50 ~ 100	100
100 ~ 300	200
300 ~ 600	300

During the process of simulative computation, the temperatures of five key points (see Fig.2) are recorded in Fig.3, from which we can find that the temperature of point 2 increases quickly up to the solidus temperature of Ti-15-3 in 100 s, then keeps constant. The temperature increasing rate of point 1 is lower than that of point 2, but faster than that of the others. The lowest is that of point 4 because that the induction-heating is weaker and the cooling intensity is higher at this position. At 260 s, the temperature of point 4 reaches the solidus temperature (1 900 K) and no longer changes.

Because of the especial position of point 2 and point 4 located at the interface between the charge and the crucible, in a certain degree, their temperature changes indicate the change of the skull thickness during the ISM process. After 250 s, their temperatures are not lower than the solidus temperature, so during the melting process, the thickness of the skull is very thin. At 250 s, the temperatures of points 0, 1 and 3 have reached a temperature (2010 K) higher than the liquidus temperature (1 920 K), then increase slowly. This indicates that the charge has been melted. After 260 s, the temperatures of points 0, 1, 3 keep at 2032 K and this indicates the equilibrium has been attained and the ultimate temperature of the melt can reach 2 032 K under the condition of 4 kg charge and 300 kW melting power.

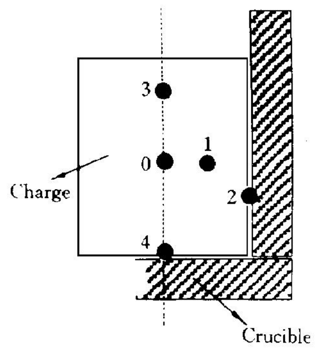

Fig.2 Schematic of key points

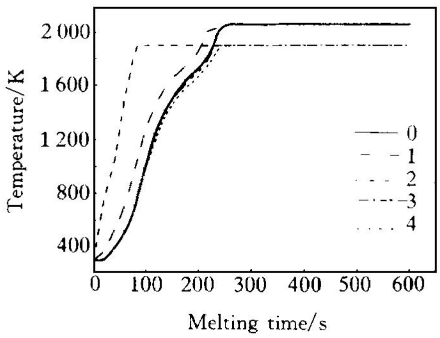

Fig.3 Temperature vs melting time of key points

3.2 Temperature distribution

In order to know the temperature distribution in the charge during the ISM process, the temperatures at different times were recorded in Fig.4. It is shown that along the radial direction, the temperature decreases sharply in the starting scope of 80 s due to the accumulation of the induction current at outside. As the melting process proceeds, the temperature in the alloy power, the charge weight. From the two figures it is very apparent that with the rise of the melting power, the melt ultimate temperature increases continuously, but with the rise of the charge weight, the melt ultimate temperature decreases. Additionally, when the melting power is lower than 125 kW and the charge is more than 4 kg, the charge cannot be melted completely and the temperatures are 1 860.6, 1 867.6 and 1 891.3 K for 5.0, 4.5 and 4.0 kg, respectively. When the melting power exceeds 150 kW, these charges with the above weights can be melted completely. In view of the superheat and the net volume of the melt, in general, the melting power of 250 to 300 kW is suitable. In this case, the super-heat can attain about 100 K and the net volume of melt is about 80 % of the original volume of the charge.

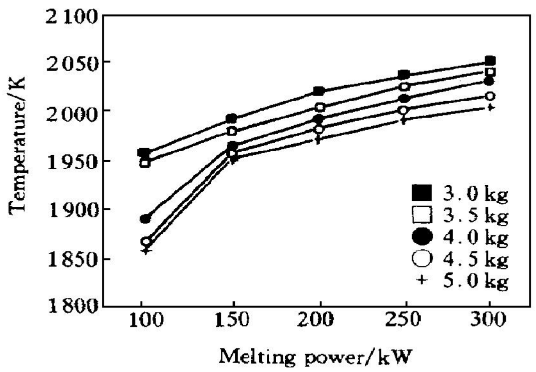

Fig.5 Influence of melting power on melt temperature

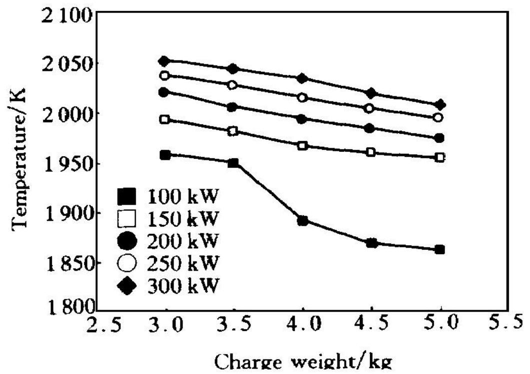

Fig.6 Influence of charge weight on melt temperature

5 CONCLUSIONS

(1) When the melting power is about 100 kW, the temperature in the surface of the charge next to the crucible quickly increases to the solidus temperature of Ti-15-3 alloy within 100 s, then keeps constant.

(2) With the rise of the melting power, the melting ultimate temperature increases continuously, but with the rise of the charge weight, the melting ultimate temperature decreases. When the melting power is lower than 125 kW and the charge is more than 4 kg, the charge cannot be melted completely. But when the melting power exceeds 150 kW, the charges with weight of 3 ~ 5 kg can be melted completely.

(3) In view of the super-heat and the net volume of the melt, in general, the melting power of 250 kW to 300 kW is suitable. In this case, the super-heat temperature can attain about 100 K and the net volume of melt is about 80 % of the original volume of the charge.

REFERENCES

1 Su Yanqing, Guo Jingjie and Jia Jun. Foundry, (in Chinese), 1997, (7): 41 - 43.

2 Su Yanqing, Guo Jingjie, Ding Hongsheng *et al*. Trans Nonferrous Met Soc China, 1998, 8(1): 69 - 72.

3 Chronister D J, Scott S W, Stickle D R *et al*. JOM, 1986, 38(9): 51 - 54.

4 Reed S. In: Kim Y-W, Wagner R and Yamaguchi M eds. TMS, 1995: 475 - 478.

5 Clites P G and Beall R A. US 3775091, 1973 - 11 - 27.

6 Sears J W. JOM, 1990, 42(3): 17 - 21.

7 Bomberger H B and Froes F H. JOM, 1984, 36 (12): 39 - 47.

8 Weber B C, Thompson W M, Bielstein H O *et al*. J American Ceramic Society, 1957, 40 (11): 363 - 373.

9 Chippereit G H. JOM, 1961, 13(2): 140 - 143.

10 Bania P. JOM, 1994, 46(7): 16 - 19.

11 Breslauer E and Rosen A. Materials Science and Technology, 1991, 7(3): 441 - 446.

(Edited by Peng Chaoqun)

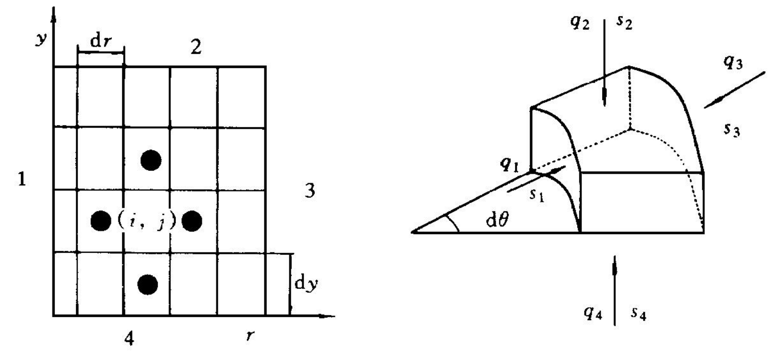

Fig.1 Controlling unit of charge

$$(\rho \cdot c \cdot V)_i \frac{T_i^{t+\Delta t} - T_i^t}{\Delta t} = \sum_{j=1}^{n} \omega(i, j) \cdot (T_j^t - T_i^t) + \frac{E}{\Delta t} + \frac{Q}{\Delta t} \quad (1)$$

$$\omega(i, j) = \frac{S(i, j)}{1/h(i, j) + L(i, j)/\lambda} \quad (2)$$

$$E = \Delta t \Sigma(\varepsilon \cdot \Gamma \cdot S)_{im}[(T_m^t + 273.15)^4 - (T_i^t + 273.15)^4] \quad (3)$$

where E —the radiant heat, J;

ρ—density of charge, $kg \cdot m^{-3}$;

c —specific heat of charge, $J \cdot kg^{-1} \cdot K^{-1}$;

V —volume of charge, m^3;

λ—thermal conductivity of charge, $W \cdot m^{-1} \cdot K^{-1}$;

Δt —time step, s;

S —area of the neighbor unit, m^2;

$L(i, j)$ —distance from unit i to unit j, m;

$h(i, j)$ —heat exchange coefficient between unit i and j, $W \cdot m^{-2} \cdot K^{-1}$;

$\omega(i, j)$ —heat resistance between unit i and j, $W \cdot K^{-1}$;

Γ—Stifen-Berlzman constant ($5.67 \times 10^{-8} W \cdot m^{-2} \cdot K^{-4}$);

ε—blackness;

Q —the heat produced by induction, J.

2.2 Boundary condition

Boundary 1 lies on the axial symmetry line, so it is heat-insulated boundary.

$$q_1 = 0 \quad (4)$$

Boundary 2 is thought as radiation boundary of that small surface (the charge surface) radiates to a big surface (inside surface of the melting chamber).

$$q_2 = 4\varepsilon \cdot \Gamma \cdot T_m^2 \quad (5)$$

$$T_m = (T - T_f)/2 \quad (6)$$

where T —melting temperature, K;

T_f —temperature of the inside surface of the melting chamber, K.

Boundary 3 has two states. Before melting, there exist the gap between the charge and the crucible wall and heat exchange is only radiation.

$$q_3 = \varepsilon \cdot \Gamma \cdot (T^4 - T_c^4) \quad (7)$$

where T_c —the temperature of crucible, K.

After melting, heat exchange depends on radiation and heat conduction (the skull contact with the crucible wall loosely).

$$q_3 = (\xi \cdot h_c + (1 - \xi) \cdot h_r) \cdot (T - T_c) \quad (8)$$

$$h_c = \frac{\lambda}{L(1, 2)} \quad (9)$$

$$h_r = \varepsilon \cdot \Gamma \cdot (T_c^2 + T^2) \cdot (T_c + T) \quad (10)$$

where h_c —heat conductivity;

h_r —heat radiation coefficient;

$L(1, 2)$ —distance between boundary unit to the crucible wall, m;

ξ—contact coefficient between the solid skull and the crucible wall.

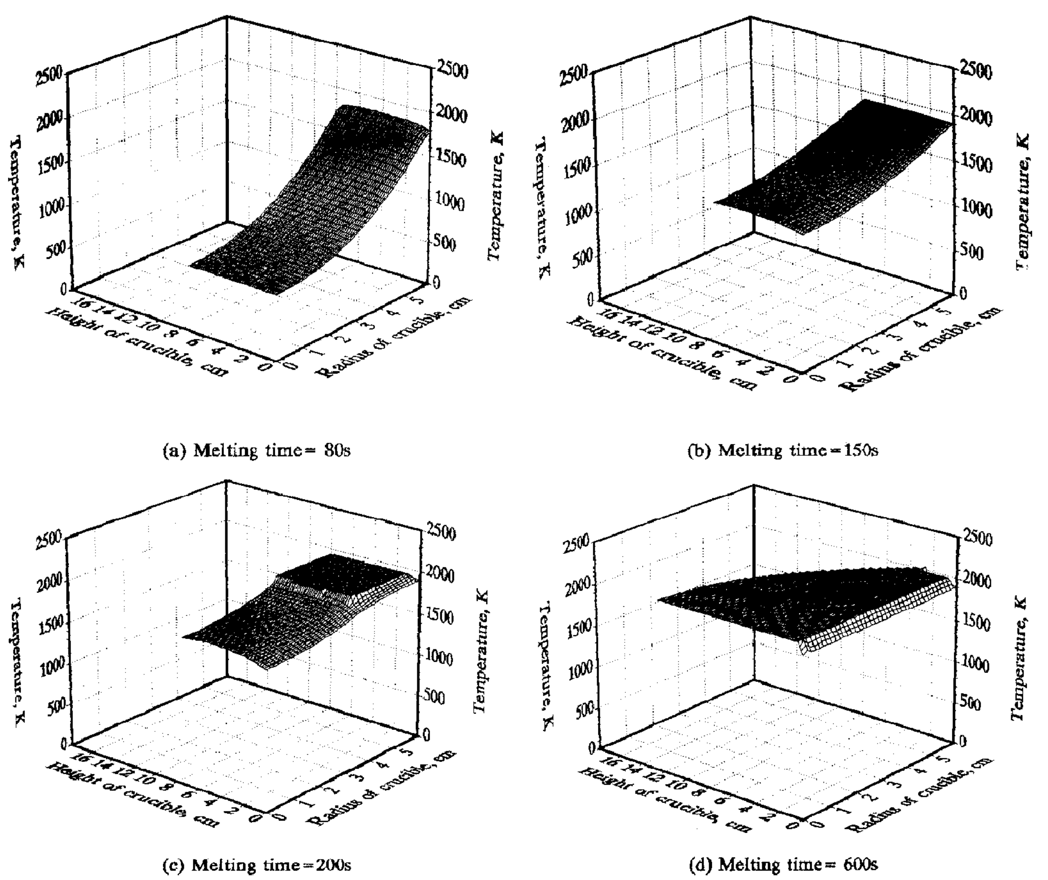

(a) Melting time = 80s
(b) Melting time = 150s
(c) Melting time = 200s
(d) Melting time = 600s

Fig.4 Temperature distribution at different times

increases and the temperature-gradient along the radial direction decreases. At 200 s, the charge has been melted into the depth of 2.7×10^{-2} m and within the melted charge there does not exist temperature-gradient due to the strong electromagnetic stirring action. At 600 s, the charge is all melted and the temperature is 2 032 K inside the melt.

The change of temperatures along the axial direction gives other information. Before the charge is not melted completely, there exists a temperature-gradient (Figs. 4(a), (b), (c)), that is, the central area has a higher temperature than the bottom and the upside of the charge. After the charge is all melted, only in the skull there exists temperature-gradient, but within the melt there does not, and at the same time, due to the appearance of electromagnetic stirring hump, the height of the melt increases from 7.5 cm to 12.2×10^{-2} m as shown in Fig.4(d).

4 OPTIMIZATION OF ISM PROCESSING PARAMETERS

As shown in Fig.3, when the melting power is 300 kW and the charge is 4 kg, the melt temperature is 2 032 K. In order to know the influence of melting power and charge weight on the melt temperature, we made the simulative computation under the conditions of different melting powers of 100, 150, 200, 250 and 300 kW and different charge weights of 3.0, 3.5, 4.0, 4.5 and 5.0 kg.

Fig.5 and Fig.6 show the relationships between the melt ultimate temperature (actually it is the temperature of point 0) and the melting